A fundamental study on the mechanistic impact of repeated de- and rehydration of $Ca(OH)_2$ on thermochemical cycling in technical scale

Sandra Afflerbach*, Reinhard Trettin

Department of Chemistry and Biology, Institute of Building and Materials Chemistry, University of Siegen, Paul-Bonatz-Strasse 9 - 11, Siegen, 57076, Germany

*Corresponding author: Tel: (+49) 2751/7404702; E-mail: afflerbach@chemie.uni-siegen.de

DOI: 10.5185/amlett.2019.2190
www.vbripress.com/aml

Abstract

A major scientific challenge for a carbon neutral, environmental friendly future energy production is the development of renewable energy production to technological readiness. One example are solar thermal power plants. Since their energy generation is intermittent, they demand for a feasible storage solution for which thermochemical reaction systems are considered. The present work subjects the thermochemical reaction system CaO / $Ca(OH)_2$ and its structural-mechanical correlations impacting the powder bulk performance upon thermochemical cycling. On exemplified $Ca(OH)_2$ crystals is shown, that during the first de- and rehydration process, the entire crystal morphology is disintegrated. The underlying mechanism is evaluated by theoretical considerations on the layered structure of $Ca(OH)_2$ and validated by scanning electron microscopy (SEM) on the probed material before and after dehydration as well as after rehydration. The obtained findings are transferred to the technically relevant powdery storage material, where they are capable to explain the phenomenon of agglomeration, which is proven by measurement of secondary particle size distribution over a number of ten thermochemical reaction cycles. From SEM imaging performed on the samples it is found, that agglomerates consist of cohering smaller particles. The inferred insights can help to deduce necessary amendments of reactor design or material modification also for other thermochemical reaction systems. Copyright © 2019 VBRI Press.

Keywords: Thermochemical energy storage, calcium hydroxide, dehydration mechanism, agglomeration, structural – mechanical correlation.

Introduction

Concentrated solar power (CSP) plants offer one option for renewable, sustainable and environmental friendly energy production by converting solar irradiance into electrical power. Especially along the Sunbelt regions of the earth, e.g. in tropical and subtropical climate zones, CSP technologies can get competitive towards other options for energy production from renewable resources as wind or geothermic. From a calculated example, 69.5 GW h/year corresponding to an average net solar yield of 44.3% could be generated from solar energy in Chuquicamata, Chile [**1**]. In comparison to photovoltaics, the advantageous potential of scale up as well as its low operating costs are seen as beneficial [**2**]. In order to overcome the intermittence of energy production from CSP plants and thus to make them capable for base load, over 70% of new plants need a feasible storage technology for an efficient operation [**3**].

Within the field of thermal storage technologies, three fundamental principles are discussed in recent literature, which are sensible, latent and thermochemical storages [**3**, **4**]. In sensible storages, which are yet the most mature, energy is stored by heating certain storage media as water or molten salts [**5**-**7**]. The amount of stored energy for these materials depends on the product of their mass and specific heat capacity. In latent storage media, energy is stored during a phase change, which can be for example from solid to liquid or solid to solid. The respective amount of stored energy therefore depends on the enthalpy of phase change, either melting and recrystallization or the transition between two solid polymorphs [**5**, **7**-**9**]. As well as for sensible as for latent thermal storages, the respective materials discharge upon cooling. Hence, a long term storage period can be associated with high parasitic costs. This drawback is overcome by thermochemical storage materials, which store and release thermal energy upon reversible chemical reactions [**7**, **10**, **11**]. During the storage process, a solid educt AB is decomposed into a solid product A and a gaseous product B, which are separated during the storage period. Hence, thermochemical systems also allow for a long term and loss free storage without generating parasitic costs during the storage period [**12**]. In case of thermochemical storage materials, the

Copyright © 2019 VBRI Press

amount of stored energy is determined by the reaction enthalpy of respective reaction systems.

Hence, in comparison to the other storage technologies, thermochemical systems have the highest storage densities of up to around 400 kw/h, however they are still the less developed and have not reached the final level of technological readiness [**13**, **14**]. Beside their potential storage density, a second crucial selection criterion of respective reaction systems is the equilibrium temperature, which has to match to the considered heat source. For CSP applications, the reaction system $Ca(OH)_2$ / CaO is one of the most considered in literature due to its cost efficiency, good availability and non-toxicity. It is based on a simple reversible gas-solid reaction with an equilibrium temperature of 505 °C at a water vapor partial pressure of 1 bar [**15**] (**Fig. 1**).

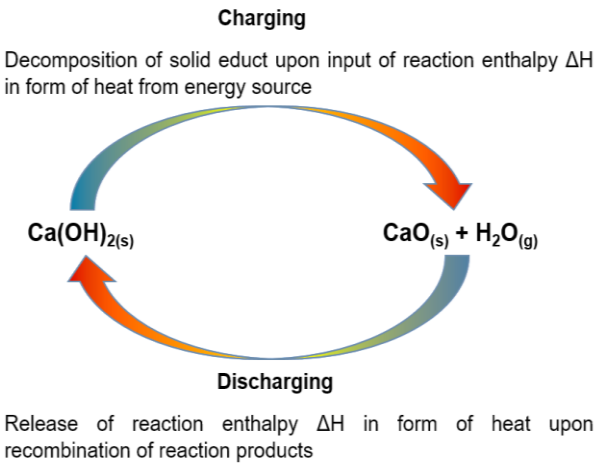

Fig. 1. The functional principle of thermochemical cycling explained on the reaction system $Ca(OH)_2$ / CaO.

While its thermodynamic properties in laboratory scale are widely investigated and entirely promising within this scope [**15**-**18**], inhomogeneities in heat and mass transport due to agglomeration effects of the powdery material upon thermochemical cycling in reactor scale are reported for fixed reaction beds [**19**, **20**]. Furthermore, due to the average particle size, mostly in the range below around 20 µm and the corresponding cohesiveness of respective powders, the material is not suitable for moved or fluidized reaction beds [**21**, **22**]. Recent investigations have shown, that the particle size is not persistent over thermochemical cycling and hence particle size stabilization approaches by additives [**20**], matrices [**23**] or semipermeable capsules [**24**] have been described in order to ensure constant bulk characteristics over a multitude of reaction cycles to which the detailed technical reactor setup can be adapted.

In sum, the discussed phenomena accompanying repeated thermochemical cycling of respective materials affect a successful technological implementation. However, an understanding of the underlying causes and mechanisms would promote technological readiness by providing a basis for the necessity and options for advanced material adaptions also for similar reaction systems. However, they have yet not been investigated.

First insights to the fundamental mechanisms can be found in literature on thermal dehydration reactions [**25**-**27**], where Galwey compared numerous reactions in order to identify a possible classification system for solid state dehydrations [**26**]. During a number of three cycles of de- and rehydration of $Ca(OH)_2$ it was found by Galwey, that the dehydration rate in laboratory scale increased with increasing number of cycles and ascribed this observation to successive crystalline disintegration [**27**]. Within a recently published molecular dynamics simulation study it was found, that the agglomeration of $Ca(OH)_2$ proceeds faster than in its charged form, CaO, and that agglomeration hinders a fast charging and discharging [**28**], what is comprehensive in terms of decreased heat and mass transport of the gaseous reaction partner through respective microstructures.

The present work provides a first experimental approach for the understanding of fundamental mechanisms accompanying multiple repeated cyclic gas-solid reactions in small reactor scale on the example of tenfold de- and rehydration of the system $Ca(OH)_2$ /CaO by probing mutual connections of primary and secondary particle size over a number of ten thermochemical cycles utilizing powdery $Ca(OH)_2$ starting material. For the initial de- and rehydration experiment, a synthetic crystal of $Ca(OH)_2$ was utilized as a model system.

Experimental

For a basic, initial experiment on the morphological changes of typical hexagonal prismatic crystals of $Ca(OH)_2$ during dehydration, macroscopic specimens were synthesized according to the method of Ashton [**29**] from aqueous solutions of $CaCl_2$ (Carl Roth, purity ≥ 98%) and NaOH (Carl Roth, purity ≥ 99%), prepared with degassed, deionized water. Dehydration was performed by dynamic heating with 5 K/min in N_2 atmosphere within a simultaneous thermal analysis apparatus (Netzsch, Jupiter 449 F3) in a platinum crucible at a maximum temperature of 480 °C. One rehydration was performed on the crystals using the described apparatus under dynamic cooling with 5 K/min to 350 °C at a water vapor partial pressure of 50 kPa in N_2.

As starting material for thermochemical cycling in small reactor scale, commercial $Ca(OH)_2$ powder from the company Heidelberger Kalk, product name Weißkalkhydrat CL90-S, with a purity of 97% was used. Basic characteristics of the material are listed in **Table 1** in the supporting material to this article.

Around 150 g of the material were cycled in a steel container filled into a quartz tube furnace, which was operated under constant flow of N_2 inert gas between 550 °C for dehydration and 350 °C for rehydration at a water vapor partial pressure of around 1 bar. The

Copyright © 2019 VBRI Press

described setup during cycling corresponds to the conditions of a small, fixed reaction bed.

From the starting material and also after each cycle of de- and rehydration the particle size distribution in the range between 0.1 to 1,000 µm has been determined using a Malvern Mastersizer Hydro2000SM. As dispersant, 2-propanol of technical quality was used. For the calculation of the results, the refractive index of the dispersant was experimentally determined using a refractometer and its value of 1.37 was entered to the accessory software (Malvern 2000). The refractive index and absorption coefficient of $Ca(OH)_2$ were taken from the instrument supplier database. In order to obtain reliable values for the secondary particle size, e.g. the size of agglomerates which may form upon thermochemical cycling of the powder, the optimal stirring rate for the measurement was determined by a previous test run to 1500 rpm. With stirring rates increasing the determined rate, a continuous decrease of particle size was observed due to disintegration of the agglomerates.

Scanning electron microscopy (SEM) was performed to qualitatively examine possible changes upon cycling in particle size distribution and morphology using a FEI Quanta FEG 250 microscope equipped with a large field detector (LFD) for secondary electron imaging, ensuring a high resolution for topographic analysis. Respective micrographs were taken in low vacuum mode (sample chamber pressure between 90 and 110 Pa) with the respective samples adhered to carbon pads.

The crystalline phase composition of the starting material and after each thermochemical cycle was determined by X-ray powder diffraction with Cu K_α radiation in a scan range between 8–75 °2θ using a Panalytical X´Pert Pro PW 3040/60 powder diffractometer with Bragg-Brentano geometry and X´Pert High Score Plus software. From Rietveld refinement performed on the obtained diffraction patterns, the crystalline and amorphous contents were determined to account for possible changes of their relation due to recrystallization processes corresponding to repeated de- and rehydration of the storage material.

Results and discussion

From the SEM micrographs taken on the basal faces {001} and lateral faces equivalent to {100} of the synthesized $Ca(OH)_2$ crystals, it can be shown, that upon dehydration a differing behavior is obtained: While on the {001} basal faces a formation of radiating cracks on the entire surface is observed, the lateral faces exhibit numerous parallel cracks of different spacings and the crystal is expanded perpendicular to the crack direction. This initial degradation of the crystal morphology is significantly intensified after rehydration, where the respective cracks initially formed upon dehydration are even more distinct (**Fig. 2**).

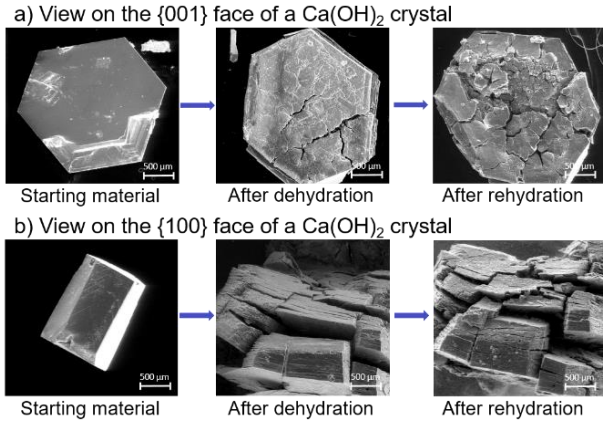

Fig. 2. SEM micrographs of synthesized $Ca(OH)_2$ crystals before dehydration, after dehydration and after rehydration taken on the crystal faces {001} (a) and {100} (b) at 100-fold magnification.

Upon heating, the internal movement of lattice constituents increases up to a point, where chemical bonds are broken and water is formed. Irrespective of the corresponding mechanism of water formation, which may proceed by a formation of protonium ions recombining with OH-groups, the formed water molecules have to leave the crystal structure. Hence, with increasing dehydration rate the water molecules cause an increasing pressure within the entire lattice inducing an expansion perpendicular to the preferred cleavage plane, running parallel to the basal face {001}. The reason for the expansion perpendicular to the preferred cleavage plane of $Ca(OH)_2$ can be found in that fact, that in this direction the weakest bonding situation in the overall structure is located, since the stacked HO-Ca-OH layers mutually cohere due to H-bonding (**Fig. 3c**). If the dehydration rate is high, and thus also the pressure increase within the lattice, additionally cracks parallel to the lateral faces may form, giving extra space in form of channels for the water molecules to escape as was stated by Galwey [**26**]. In sum, this process leads to a formation of small flinders and a residual, larger crystal which now provides an increased surface area and a decreased mechanical stability, promoting a fast rehydration reaction in the presence of water vapor upon cooling as described by Galwey [**27**] (**Fig. 3**).

When rehydration is initiated, $Ca(OH)_2$ crystals are firstly formed on the available surface of the dehydrated phase, where both reactants, the CaO surface and H_2O molecules come into contact, forming an interfacial reaction zone. Dependent on the specific relation of nucleation speed to the growth rate of the nuclei, which could be adjusted by the concentration of water vapor in the N_2 purge gas, the growing $Ca(OH)_2$ crystals shift the previously cracked and destabilized fragments of the remained, larger crystal apart and thereby the crystals fragmentation proceeds (**Fig. 2**).

From the results and considerations discussed above, it is evident, that in case of crystals of comparable size repeated de- and rehydration leads to a decreasing crystallite size and therefore an overall

Copyright © 2019 VBRI Press

increased specific surface area within the first reaction cycles. Hence, it seems probable that there could be an adjustment of equilibrium crystallite size upon thermochemical cycling, depending on the applied conditions as for example water vapor pressure, which is obtained after a defined number of reaction cycles. It is conceivable, that this equilibrium size would be in a range significantly below 100 µm, as obtained in corresponding commercial powders. However, this hypothesis cannot be finally proven from the results in the present work but gives rise to plans for future investigations.

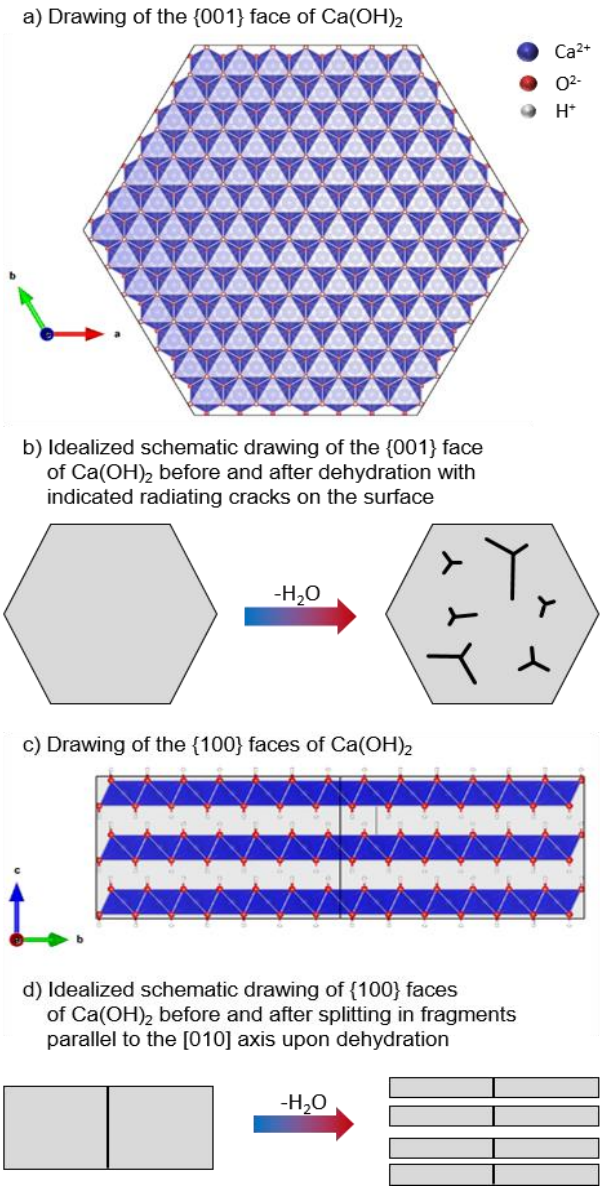

Fig. 3. Drawings of the lattice structure of $Ca(OH)_2$ within a typical hexagonal prismatic crystal (a) and (c), both drawn with VESTA [**30**] with schematic illustrations of the crack formation upon dehydration (b) and (d).

In case of common investigations on thermochemical cyclability performed on the material in laboratory and technical scale, usually directly commercial $Ca(OH)_2$ powders are utilized, since this would be the appropriate form of the material to be implemented within future technical setups. However, the results obtained from the fundamental experiment described above are also of relevance for an understanding of the behavior of the powdery starting material upon thermochemical cycling.

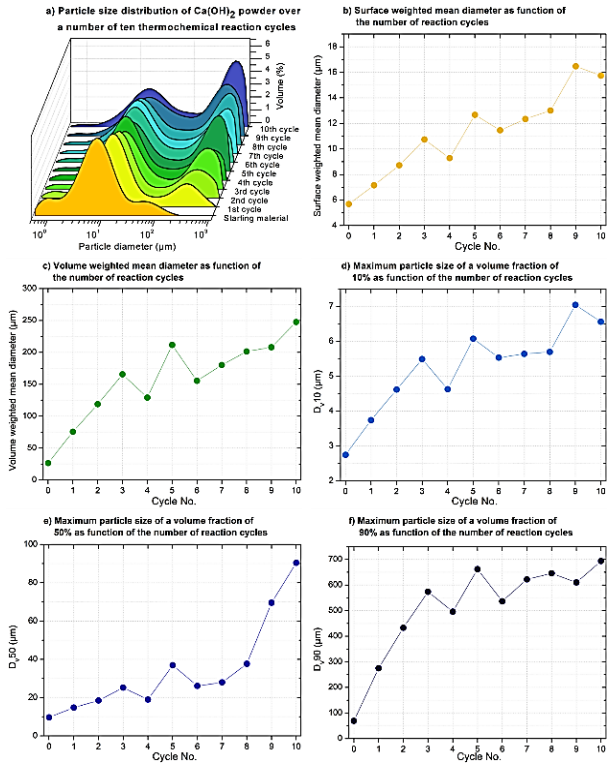

Fig. 4. Particle size distribution of a powder sample of $Ca(OH)_2$ before and after each out of ten thermochemical reaction cycles; a) Plot of volumetric particle size distribution; b) Trend of surface weighted mean diameter; c) Trend of volume weighted mean diameter; d) Trend of D_v10 diameter; e) Trend of D_v50 diameter; f) Trend of D_v90 diameter.

Since the crystallite size and hence the primary particle size is accessible to a reliable determination by a calculation of the scattering domain size only in a range up to 500 nm, it could not be determined on the powdery material used in this work. Yet, the particle diameter corresponding to the secondary particle size has been determined by laser granulometry. From the obtained results it can be qualitatively observed, that the amount of particles within the main fraction of particle diameter around 6 µm tends to an increase in diameter and to a decrease of its amount upon repeated thermochemical cycling. Simultaneously, the amount of fines with a diameter below 2 µm is continuously decreasing with increasing cycling number. In contrast, the fraction of larger particles with a particle diameter around 70 µm is increasing during repeated thermochemical cycling (**Fig. 4a**).

A more profound analysis of the trends for changes in particle size can be made by monitoring separated sections of size, calculated as mean diameters or percentile fractions below a certain size limit.

Copyright © 2019 VBRI Press

The surface weighted mean (also called Sauter mean diameter), which is particularly suitable for describing changes of fines, shows an almost continuous increase of particle diameters from 5.7 µm for the starting material to 15.8 µm for the material measured after ten thermochemical reaction cycles, what corresponds roughly to a triple of the initial value (**Fig. 4b**).

Similarly, also the volume weighted mean (called de Brouckere mean diameter), feasible for an evaluation of the bulk of particles, increases from initially 26.3 µm for the starting material to 247.6 µm after a number of ten thermochemical cycles of de- and rehydration, which is around nine times higher as the value determined for the starting material (**Fig. 4c**).

In contrast to this overall continuous increase, which is also found for the fraction of smallest particles, determined as the D_v10 (**Fig. 4d**), the medium diameter fraction D_v50 shows only a slight increase in size up to the fourth reaction cycle from 9.7 µm to 19.0 µm. From the seventh thermochemical cycle on, the D_v50 diameter significantly increases to a value of 90.4 µm, corresponding to a tenfold multiplication of the initial value (**Fig. 4e**).

For the largest particles of the investigated bulk material, determined as the D_v90 diameters, a continuous increase of the measured diameters is found from the first reaction cycle on and the trend is continued up to the third cycle, from which the diameters oscillate between 495.9 µm and 693.5 µm. After a number of three initial cycles, the diameter significantly increases from 69.2 µm to 432.9 µm (**Fig. 4f**).

In sum, the observed results validate the overall trend for the particles of the thermochemical reaction system $CaO / Ca(OH)_2$ to agglomerate upon thermochemical cycling. Not only in large scale reactors, as commonly described in recent works, but even in a small scale with a loose powder filling as it was performed in the present work.

According the classification from Geldart [**21**, **22**], respective powders with a mean diameter above 20 µm should be fluidizable.

However, in experimental works on the investigated reaction system, a fluidization is not successful.

When looking at the SEM micrographs taken on the cycled material investigated in the present work, this observation can be explained by the structural nature of the respective particles. Before cycling as well as after a number of five and ten thermochemical cycles, agglomerates of different size are observable. However, from the SEM micrographs taken at a 10,000 fold magnification it can be proven that the individual agglomerates consist of numerous, cohering smaller particles. This observation is especially valid for the cycled material. From this result it is conceivable, that upon movement or fluidization the agglomerates structurally degenerate due to the mechanical forces applied to them, thereby recreating fines, predominantly with diameters below the value of 20 µm (**Fig. 5**).

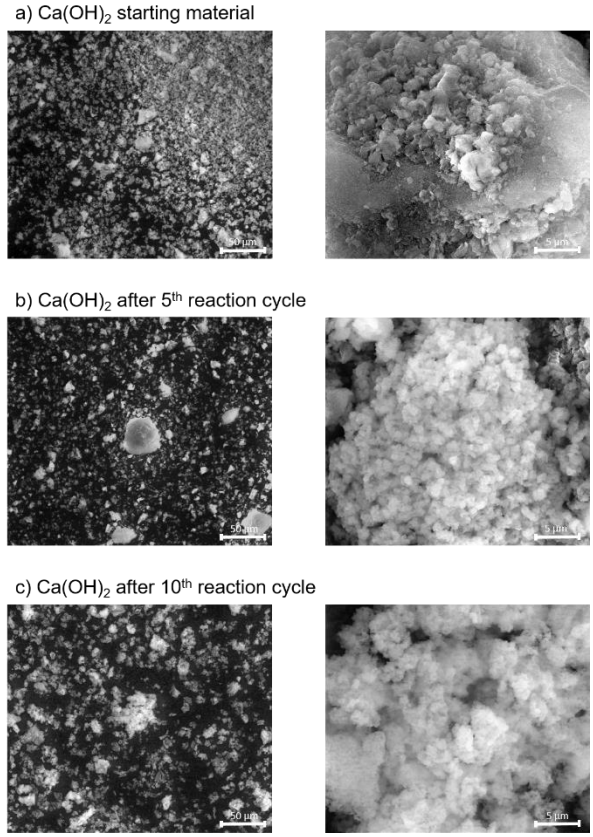

Fig. 5. SEM micrographs of $Ca(OH)_2$ powder; a) Starting material; b) After five and c) after reaction cycles at 1,000-fold magnification (left) and 10,000-fold magnification (right).

Transferring the observations made on the synthesized $Ca(OH)_2$ crystal, which degenerates upon de- and rehydration into flinders (compare **Fig. 2** and **Fig. 3**), it is consistent, that also in case of the cycled powdery material the contained crystallites degenerate into smaller individuals, accompanied by a corresponding tremendous increase of the surface area. Hence, the ratio of surface free energy to volume free energy is also significantly increased as well as corresponding interparticular forces, which in consequence lead to the observed agglomeration effect. In case of the reaction system $CaO / Ca(OH)_2$, this effect is especially pronounced by the possibility of the formation of H-bonds between adjacent particles which add to the interparticular coherency beside their electrostatic interactions.

In order account for possible effects of the repeated recrystallization effects during thermochemical cycling on the crystallinity of the investigated sample, the phase composition of the specimen was determined for the starting material and after each reaction cycle (**Fig. 6**). The initial sample has a content of 71 (%w/w) of crystalline $Ca(OH)_2$, while 29 (%w/w) of the storage material are X-ray amorphous. Since the utilized material has a purity of 97%, it is evident that a certain amount of $Ca(OH)_2$ crystallites within the overall

Copyright © 2019 VBRI Press

material are too small to contribute to diffraction and hence appear as part of the amorphous phase content. After the first reaction cycle, the crystalline phase is significantly reduced to a value of 45.6 (%w/w) and increases afterwards to a value around 63 (%w/w). From the eighth reaction cycle on, the crystallinity of $Ca(OH)_2$ is again decreased to 52 (%w/w). Minor contents of $CaCO_3$ detected in all samples are ascribed to the carbonization of $Ca(OH)_2$ during sample cycling, preparation or measurement.

Considering the results obtained from X-ray diffraction, additional proof is found for the interpretation of the previous results, as it is obvious, that an dynamic equilibrium crystallinity is obtained during thermochemical cycling with values between 63 (%w/w) and 52 (%w/w). While a certain level of crystallinity is retained for the crystallites as the primary particles, the size of agglomerates formed by them is increasing upon cycling until a certain level is reached for the fraction with the highest diameters, e.g. the D_v90 values (compare **Fig. 4f**).

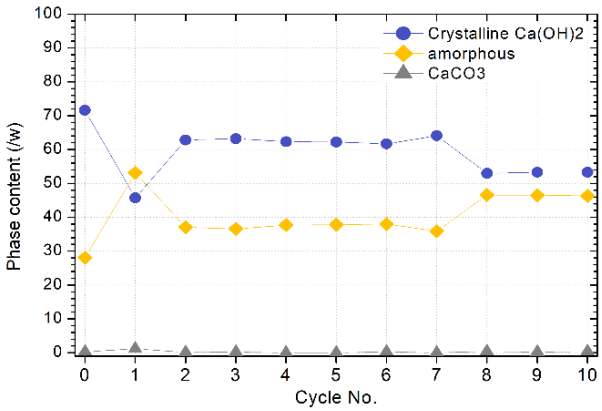

Fig. 6. Phase contents of the $Ca(OH)_2$ powdery starting material and after each out of ten thermochemical reaction cycles.

Conclusion

From a fundamental approach on the mechanistic impact on the de- and rehydration of synthesized $Ca(OH)_2$ crystals, the experimentally observed degradation process can be related to the internal crystal structure of the material. Thereby it is found, that the respective crystal is fanned out perpendicular to its preferred cleavage plane, which runs parallel to the basal face {001}. Radiating cracks formed on the basal faces, give additional space for water formed during dehydration to escape. During rehydration, the initial educt is retained on the significantly increased surface area of the cracked crystal. From recrystallization of $Ca(OH)_2$, the degradation of the overall structure is promoted and the initial crystal is disintegrated into fragments. These interrelations pronounce the importance of the structural nature of a material for its performance upon repeated de- and rehydration accompanying thermochemical cycling.

The findings are transferred to the technically relevant storage material of powdery form, for which a significant agglomeration tendency upon cycling is proven. While the size of the primary particles, e.g. crystallites, is reduced, the size of the secondary particles, e.g. agglomerates, is increased. This phenomenon is ascribed to the increased surface free energy to volume free energy ratio, which enhances the interparticular interaction. Additionally, the formation of H-bonds may contribute to the overall coherency between individual crystallites within an agglomerate lump. During thermochemical cycling, within a certain range a defined level of the ratio of crystalline to amorphous is reached, pointing to a dynamic equilibrium for recrystallization processes accompanying de- and rehydration.

In sum, these structural - mechanical relations justify future investigations also on other reaction systems suitable for thermochemical energy storage, as the results are capable to provide important insights for technical adaptions of reactor design or allow a decision on the necessity of advanced material modifications on the pathway to technological readiness. On the example of the subjected reaction system $CaO / Ca(OH)_2$, recently published approaches for particle size stabilization should be mentioned [**20**, **23**, **24**, **31**, **32**]. However, in this context, fundamental mechanistic investigations and simulations on repeated de- and rehydration reactions would significantly add to a general understanding of the relation of structural features to functionality, properties and performance, which could in turn be also of highest value for other processes involving gas-solid reactions as for example the recycling of certain building materials or materials used for chemical looping combustion.

Acknowledgements

This work was supported by the European Union within the 7th Framework Program, ENERGY.2011.2.5-1, project number 282889, for which the authors gratefully acknowledge.

Author's contributions

Conceived the plan: S. A.; Performed the experiments: S. A.; Data analysis: S. A.; Wrote the paper: S. A.; Discussion partner: R. T. Authors have no competing financial interests.

Supporting information

Supporting informations are available from VBRI Press.

References

1. Zhang, H. L.; Baeyens, J.; Degrève, J.; Cacères, G., *Renewable Sustainable Energy Rev.*, **2013**, *22*, 466, **DOI:** 10.1016/j.rser.2013.01.032
2. Desideri, U.; Campana, P. E., *Appl. Energy*, **2014**, *113*, 422. **DOI:** 10.1016/j.apenergy.2013.07.046
3. Pelay, U.; Luo, L.; Fan, Y.; Stitou, D.; Rood, M., *Renewable Sustainable Energy Rev.*, **2017**, *79*, 82. **DOI:** 10.1016/j.rser.2017.03.139
4. Garg, H. P.; Mullick, S. C.; Bhargava, A. K., Solar Thermal Energy Storage; Springer Netherlands**:** Dordrecht, **1985**.
5. Alva, G.; Lin, Y.; Fang, G., *Energy*, **2018**, *144*, 341. **DOI:** 10.1016/j.energy.2017.12.037
6. Li, G.; Zheng, X., *Renewable Sustainable Energy Rev.*, **2016**, *62*, 736. **DOI:** 10.1016/j.rser.2016.04.076

Copyright © 2019 VBRI Press

7. Haider, M.; Werner, A., *Elektrotechnik & Informationstechnik*., **2013**, *130*, 153. **DOI:** 10.1007/s00502-013-0151-3
8. Li, G., *Renewable Sustainable Energy Rev.*, **2015**, *51*, 926. **DOI:** 10.1016/j.rser.2015.06.052
9. Sharma, S. D.; Sagara, K., *Int. J. Green Energy*, **2005**, 2, 1. **DOI:** 10.1081/GE-200051299
10. Abedin, A. H., *TOREJ*, **2011**, *4*, 42. **DOI:** 10.2174/1876387101004010042
11. Aydin, D.; Casey, S. P.; Riffat, S., *Renewable Sustainable Energy Rev.*, **2015**, *41*, 356. **DOI:** 10.1016/j.rser.2014.08.054
12. Michel, B.; Mazet, N.; Mauran, S.; Stitou, D.; Xu, J., *Energy*, **2012**, *47*, 553. **DOI:** 10.1016/j.energy.2012.09.029
13. Prieto, C.; Cooper, P.; Fernández, A. I.; Cabeza, L. F., *Renewable Sustainable Energy Rev.*, **2016**, *60*, 909. **DOI:** 10.1016/j.rser.2015.12.364
14. Cot-Gores, J.; Castell, A.; Cabeza, L. F., *Renewable Sustainable Energy Rev.*, **2012**, *16*, 5207. **DOI:** 10.1016/j.rser.2012.04.007
15. Schaube, F.; Koch, L.; Wörner, A.; Müller-Steinhagen, H., *Thermochim. Acta*, **2012**, *538*, 9. **DOI:** 10.1016/j.tca.2012.03.003
16. Schaube, F.; Kohzer, A.; Schütz, J.; Wörner, A.; Müller-Steinhagen, H., *Chem. Eng. Res. Des.*, **2013**, *91*, 856. **DOI:** 10.1016/j.cherd.2012.09.020
17. Criado, Y. A.; Alonso, M.; Abanades, J. C., *Ind. Eng. Chem. Res.*, **2014**, *53*, 12594. **DOI:** 10.1021/ie404246p
18. Pardo, P.; Anxionnaz-Minvielle, Z.; Rougé, S.; Cognet, P.; Cabassud, M., *Sol. Energy*, **2014**, *107*, 605. **DOI:** 10.1016/j.solener.2014.06.010
19. Roßkopf, C.; Haas, M.; Faik, A.; Linder, M.; Wörner, A., *Energ. Convers. Manage.*, **2014**, *86*, 93. **DOI:** 10.1016/j.enconman.2014.05.017
20. Roßkopf, C.; Afflerbach, S.; Schmidt, M.; Görtz, B.; Kowald, T.; Linder, M.; Trettin, R., *Energ. Convers. Manage.*, **2015**, *97*, 94. **DOI:** 10.1016/j.enconman.2015.03.034
21. Geldart, D., *Powder Technol.*, **1973**, *7*, 285. **DOI:** 10.1016/0032-5910(73)80037-3
22. Geldart, D.; Harnby, N.; Wong, A. C., *Powder Technol.*, **1984**, *37*, 25. **DOI:** 10.1016/0032-5910(84)80003-0
23. Álvarez Criado, Y.; Alonso, M.; Abanades, J. C., *Ind. Eng. Chem. Res.*, **2015**, *54*, 9314. **DOI:** 10.1021/acs.iecr.5b02688
24. Afflerbach, S.; Kappes, M.; Gipperich, A.; Trettin, R.; Krumm, W., *Sol. Energy*, **2017**, *148*, 1. **DOI:** 10.1016/j.solener.2017.03.074
25. L'vov, B. V. Thermal Decomposition of Solids and Melts. New Thermochemical Approach to the Mechanism, Kinetics and Methodology; Springer Netherlands**:** Dordrecht, **2007**. **DOI:** 10.1016/j.sab.2010.09.009
26. Galwey, A. K., *Thermochim. Acta*, **2000**, *355*, 181. **DOI:** 10.1016/S0040-6031(00)00448-2
27. Galwey, A. K.; Laverty, G. M., *Thermochim. Acta*, **1993**, *228*, 359. **DOI:** 10.1016/0040-6031(93)80304-S
28. Xu, M.; Huai, X.; Cai, J., *J. Phys. Chem. C*, **2017**, *121*, 3025. **DOI:** 10.1021/acs.jpcc.6b08615
29. Ashton, F. W. ; Wilson, R., *Am. J. Sci.*, **1927**, *5*, 209. **DOI:** 10.2475/ajs.s5-13.75.209
30. Momma, K.; Izumi, F., *J. Appl. Crystallogr.*, **2011**, *44*, 1272. **DOI:** 10.1107/S0021889811038970
31. Benitez-Guerrero, M.; Valverde, J. M.; Perejon, A.; Sanchez-Jimenez, P. E.; Perez-Maqueda, L. A., *Appl. Energy*, **2018**, *210*, 108. **DOI:** 10.1016/j.apenergy.2017.10.109
32. Korhammer, K.; Druske, M.-M.; Fopah-Lele, A.; Rammelberg, H. U.; Wegscheider, N.; Opel, O.; Osterland, T.; Ruck, W., *Appl. Energy*, **2016**, *162*, 1462. **DOI:** 10.1016/j.apenergy.2015.08.037

Copyright © 2019 VBRI Press